

A lanthanide metal-organic framework based on a custom-designed macrocyclic ligand

Chavis A. Stackhouse, Wen-yang Gao, Lukasz Wojitas, Weijie Zhang & Shengqian Ma

To cite this article: Chavis A. Stackhouse, Wen-yang Gao, Lukasz Wojitas, Weijie Zhang & Shengqian Ma (2016) A lanthanide metal-organic framework based on a custom-designed macrocyclic ligand, *Journal of Coordination Chemistry*, 69:11-13, 1844-1851, DOI: 10.1080/00958972.2016.1194979

To link to this article: <http://dx.doi.org/10.1080/00958972.2016.1194979>



View supplementary material [↗](#)



Accepted author version posted online: 01 Jun 2016.
Published online: 13 Jun 2016.



Submit your article to this journal [↗](#)



Article views: 31



View related articles [↗](#)



View Crossmark data [↗](#)

A lanthanide metal-organic framework based on a custom-designed macrocyclic ligand

Chavis A. Stackhouse, Wen-yang Gao, Lukasz Wojtys, Weijie Zhang and Shengqian Ma

Department of Chemistry, University of South Florida, Tampa, FL, USA

ABSTRACT

The lanthanum-based metal macrocyclic framework, MMCF-3, where the ligand is 1,4,7,10-tetraazacyclododecane-*N,N',N'',N'''*-tetra-*p*-methylbenzoic acid, has been synthesized and characterized by powder X-ray diffraction, single crystal X-ray diffraction, and thermogravimetric analysis. MMCF-3 forms in closely packed 2-D sheets. In MMCF-3, the azamacrocyclic-based ligand coordinates tetradentate to four separate lanthanum ions via its carboxylate groups, leaving the macrocycle site unoccupied. The lanthanum ions are 10-coordinate with a distorted bi-capped square anti-prism coordination environment. The vacancy of the macrocycle site within the framework encourages the utilization of the framework as a cation receptor. The availability of these sites allows for the possibility to coordinate to newly introduced metals to produce heterometallic frameworks, which could exhibit intriguing properties.

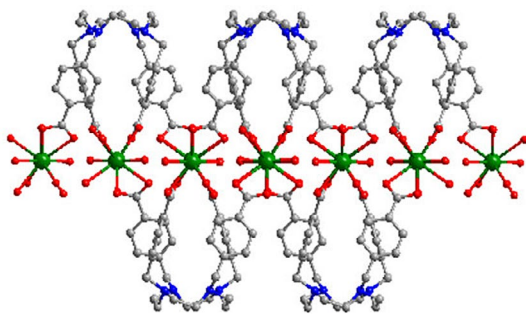
ARTICLE HISTORY

Received 10 February 2016

Accepted 23 May 2016

KEYWORDS

Azamacrocycles; cyclen; lanthanide; metal-organic frameworks



1. Introduction

Research in metal-organic frameworks (MOFs) has risen in recent decades due to their unequalled potential tunability and structural diversity [1]. MOFs may be described as crystalline structures composed of metal cations or clusters of cations, commonly referred to as secondary building units (SBUs), and custom-designed organic ligands [2]. The variety of structural motifs, ligands, and SBUs that may be incorporated promote the attainment of essentially countless potential MOFs and application in numerous areas of interest, such as gas adsorption, catalysis, gas separation, and sensing [3–5]. Implementation of these materials in sensing arises from the frameworks' ability to increase the concentration of a

CONTACT Shengqian Ma  sqma@usf.edu

 Supplemental data for this article can be accessed at <http://dx.doi.org/10.1080/00958972.2016.1194979>.

© 2016 Informa UK Limited, trading as Taylor & Francis Group

desired analyte to a greater degree than its overall presence within the system, imparting an inherent sensitivity to the aforementioned analyte. MOF materials also possess the potential for selectivity for specific analytes or classes of analytes through mechanisms such as size exclusion (molecular sieving), chemically specific interactions between the adsorbate and framework, and the directed design of pore and aperture size through selection of appropriate organic linkers or struts [4].

Polyazamacrocycles represent a popular class of macrocyclic ligands for supramolecular chemistry and crystal engineering. This popularity may be due to the complexes' high thermodynamic stability, relative kinetic inertness, basicity, transition metal-ion coordinating ability, and rigid structure [6]. Furthermore, their utilization promotes network topologies as coordination in complexes containing tetradentate azamacrocycles generally produces only two isomers differing via the coordination ligand's conformation. Equatorial N_4 coordination of the macrocycle allows for interaction at the two vacant *trans*-axial positions, while the folded conformations permit interaction at two vacant *cis* positions [7]. Azamacrocycles differ from those of other classes of macrocycles due to the fact the macrocyclic cavity is commonly occupied by metal cations [8]. Materials containing azamacrocycles have found use in applications such as bleaching, oxidative catalysis [9], and molecular recognition. Cyclen units have been incorporated to construct pH-dependent selective receptors for copper(II) [10], zinc(II) [11], yttrium(III), and lanthanum(III) ions [12].

In our previous work, we employed a custom-designed macrocyclic tetracarboxylate ligand, 1,4,7,10-tetraazacyclododecane- N,N',N'',N''' -tetra-*p*-methylbenzoic acid (tactmb) (figure 1), to construct metal macrocyclic frameworks (MMCFs) for applications in carbon capture [13(a)], chemical fixation of CO_2 [13(b)], and catalysis [13(c)]. The tactmb molecule represents a flexible azamacrocyclic ligand potentially applicable to activation of small molecules, ion recognition, and capture [13]. The aforementioned ligand combined the coordination diversity of carboxylate linkers with the advantages of flexible macrocycles. Given the need for new sensors and the advantages of MOF materials, we embarked upon pursuit of materials based on the tactmb ligand and other polyazamacrocyclic ligands, which could present potential for small molecule recognition. Herein, we describe the synthesis and characterizations of a new lanthanide framework, $La(C_{40}H_{40}N_4O_8)(NH_2(CH_2)_2NO_3)$ or MMCF-3, that is constructed from the tactmb ligand and lanthanum ions.

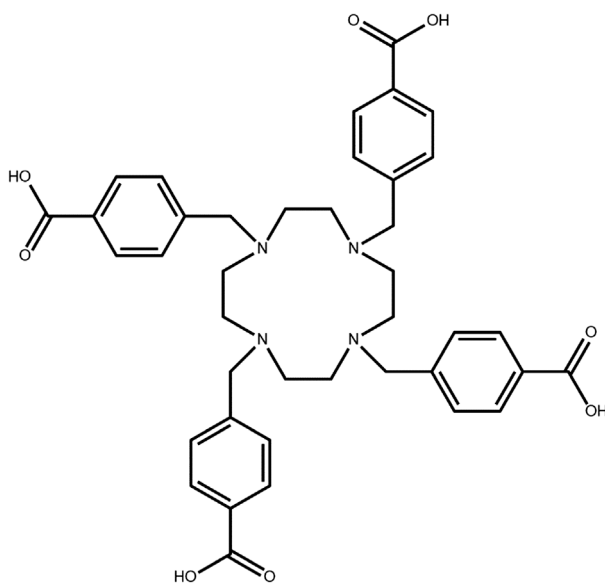


Figure 1. 1,4,7,10-Tetraazacyclododecane- N,N',N'',N''' -tetra-*p*-methylbenzoic acid (tactmb).

2. Experimental

2.1. Materials and instrumentations

Commercially available reagents were purchased as high purity from Fisher Scientific or Sigma-Aldrich and used without purification. Thermogravimetric analysis (TGA) was performed under nitrogen on a TA Instrument TGA 2950 Hi-Res from 30 to 700 °C at 10 °C min⁻¹. FTIR spectra were conducted on a PerkinElmer Spectrum Two FTIR instrument from 4000 to 500 cm⁻¹. Powder X-ray diffraction (PXRD) data for MMCF-3 were collected using a Bruker D8 Advance, CuK_α, λ = 1.54178 Å (40 kV, 40 mA) from 5° to 30° (2θ) and a step of 0.5 s/0.02° (2θ).

2.2. Syntheses of H₄tactmb and MMCF-3

2.2.1. Synthesis of H₄tactmb

The preparation of H₄tactmb may be achieved via previously reported method [13] (Supplementary Material). Yield of Tactmb: 60%.

2.2.2. Synthesis of MMCF-3

A mixture of La(NO₃)₃·H₂O (2.0 mg, 0.0058 mmol) and H₄tactmb (5.0 mg, 0.0071 mmol) in 1.0 mL solution of N,N'-dimethylformamide, isopropanol, and water (69.5:17.4:13.1%, respectively) had its pH adjusted to 5.0 using nitric acid and triethylamine. The mixture was then loaded into a Pyrex tube, sealed under

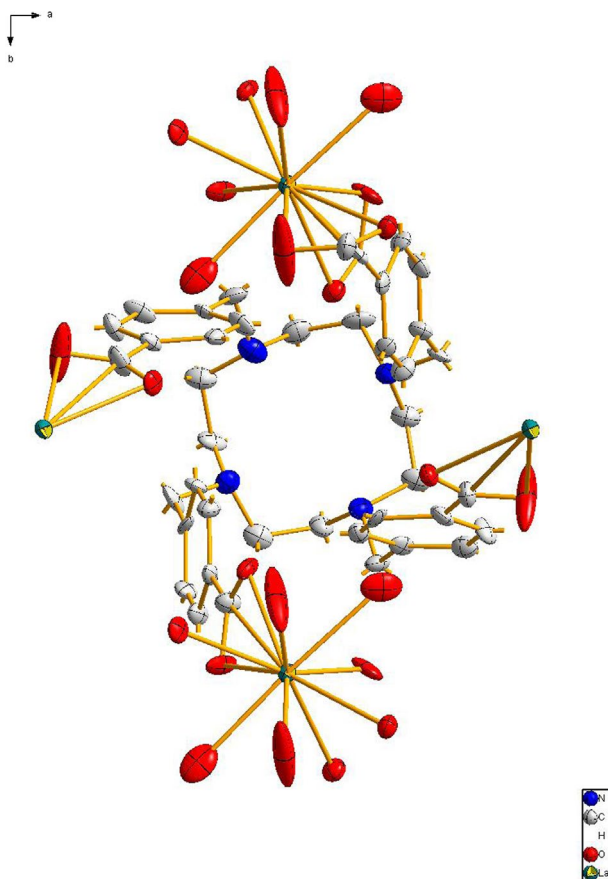


Figure 2. Asymmetric unit of MMCF-3.

vacuum, and heated to 120 °C for two weeks. The resulting colorless sheet crystals were obtained (yield: 8.0% based upon ligand).

2.3. X-ray crystallography and data collection

The X-ray diffraction data were collected using synchrotron radiation ($\lambda = 0.518 \text{ \AA}$) at Advanced Photon Source Beamline 15-ID-B of ChemMatCARS in Argonne National Lab, Argonne, IL. Indexing was performed using APEX2 [14] (Difference Vectors method). Data integration and reduction were performed using SaintPlus 6.01 [15]. Absorption correction was performed by multiscan method implemented in SADABS [16]. Space groups were determined using XPREP implemented in APEX2 [14]. The structure was solved using SHELXS-97 (direct methods) and was refined using SHELXL-2015 [17(b)] (full-matrix least squares on F^2) through OLEX2 interface program [18]. All non-disordered non-hydrogen atoms were refined anisotropically. Hydrogens of $-\text{CH}$ and $-\text{CH}_2$ groups were placed in geometrically calculated positions and were included in the refinement process using a riding model with isotropic thermal parameters: $U_{\text{iso}}(\text{H}) = 1.2 U_{\text{eq}}(-\text{CH}, -\text{CH}_2)$. Counterions were refined using geometry restraints (default esds) which were not violated in final steps of the refinement. The data were additionally contaminated by minor twinning, and pseudotranslational effects (C-centering) are present.

2.4 Gas adsorption experiments

Gas adsorption isotherms of MMCF-3 were collected using the surface area analyzer ASAP-2020. Before the measurements, the freshly prepared samples were exchanged with methanol for 3 days and then

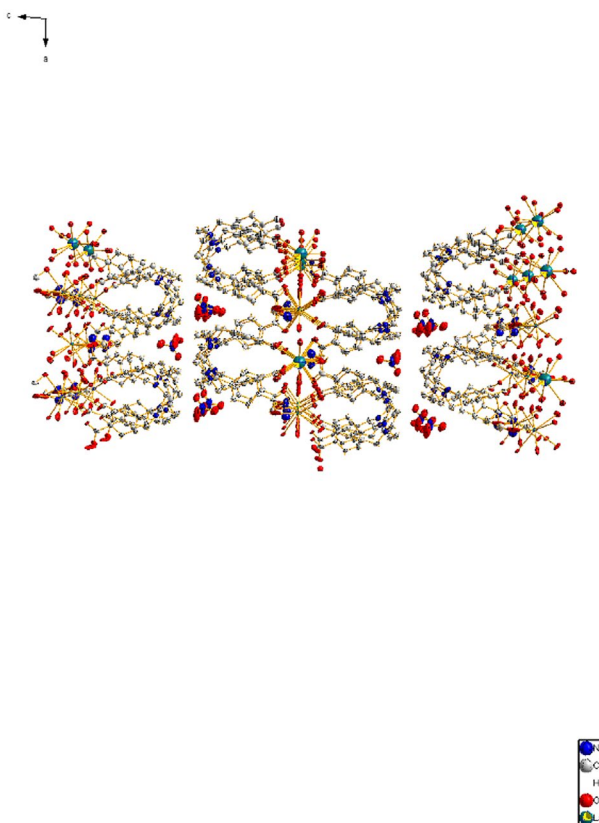


Figure 3. MMCF-3 framework as viewed along the b -axis.

activated with supercritical CO₂ in a Tousimis Samdri PVT-3-D critical point dryer. CO₂ gas adsorption isotherms were collected at 195 K using a liquid acetone–dry ice bath.

3. Results and discussion

3.1. Crystal structure description

Transparent crystals of MMCF-3 (figure 2) formed in 2-D sheets which were obtained via the reaction of tactmb with lanthanum nitrate in a solution of DMF, isopropanol, and water (8 : 1.5 : 1) at pH 5, adjusted using triethylamine and nitric acid. Single crystal X-ray diffraction reveals that MMCF-3 crystallizes under space group $P2_1$. The asymmetric unit of MMCF-3 contains one lanthanum cation, one tactmb, and two coordinated waters. There are two cavities in the asymmetric unit that are most likely filled with disordered cation (NH₂(CH₃)₂⁺, product of DMF decomposition), and NO₃⁻. This is suggested by analysis of q-peak heights and distances as well as Platon's [19] estimate of electron count in those structural voids. Considering the presence of those two counterions and lack of other voids, it was tentatively concluded that the ligand is singly protonated to balance the charge in the structure. Each La(III) is 10-coordinate with a distorted bi-capped square antiprism coordination environment formed by eight oxygens of four carboxylate groups of four separate tactmb ligands and two coordinated water molecules, one at each axial position in a *trans* fashion. The overall framework exists as stacked, distinct disjointed layers (figure 3), wherein each tactmb macrocycle ligand links with four 10-coordinate lanthanum ions. Each

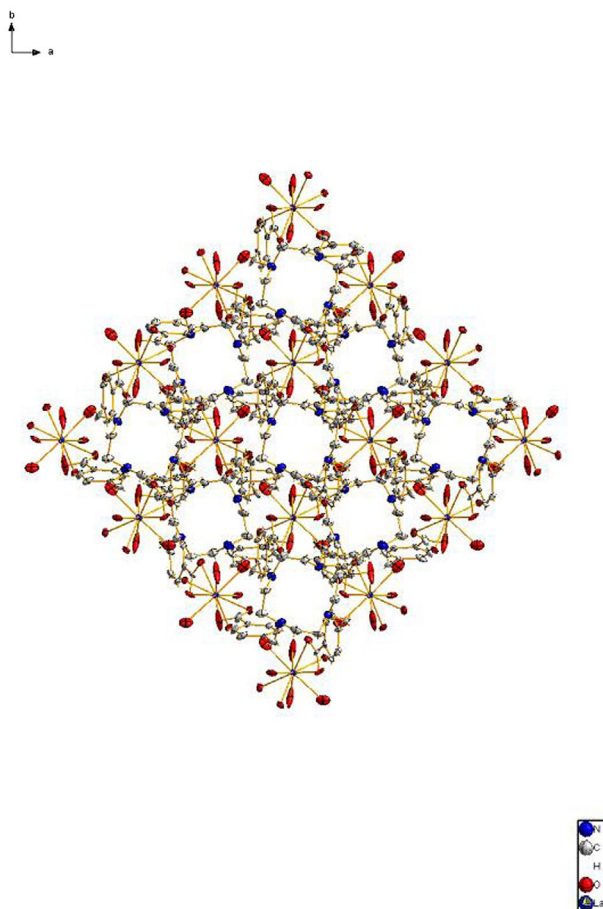


Figure 4. MMCF-3 framework as viewed along the *c*-axis.

separate layer is composed of three sublayers; one lanthanum cation bounded on either side by a layer of tactmb molecules. The lanthanide cation coordinates to carboxylate groups from two separate tactmb ligands with each of the surrounding layers. The tactmb ligands coordinate to La³⁺ via the carboxylate moieties exclusively; retaining a vacant macrocycle site then may be employed for further coordination to cations. The vacant macrocycle imparts a honeycomb esthetic to the framework layers to which all porosity in the material may be attributed (figure 4). Crystal data and refinement conditions are shown in table 1, and bond distances and angles in table 2.

3.2. Characterization of MMCF-3

The phase purity of MMCF-3 was verified by PXRD studies, which evince that the diffraction patterns of the fresh sample are consistent with the calculated pattern (Supporting Material, figure S1). PXRD studies of both the fresh and solvent-free MMCF-3 showed minute differences after solvent evacuation. This may suggest the presence of a “breathing” property indicative of some MOFs employing flexible linkers. Thermogravimetric analysis on freshly prepared MMCF-3 (figure S2) depicts a weight loss of 39%, corresponding to the loss of solvent molecules and coordinated water molecules, and the graph then plateaus until around 360 °C before complete degradation of the framework. The solvent-free MMCF-3 confirmed a plateau up to 360 °C, demonstrating moderate thermal stability of the framework. IR spectra of MMCF-3 show disappearance of the very broad peak associated with an O–H stretch ($\nu_{\text{O-H}} = 3300 \text{ cm}^{-1}$). The absence of the alcohol stretch, in comparison with the tactmb spectra, is consistent with deprotonation of the carboxylate group which occurs during solvothermal conditions and confirmed through the crystallographic data. The MMCF-3 spectra depict a shift of the peak frequency associated with the tactmb carbonyl from 1699 to 1573 cm^{-1} . This shift, indicative of a carbonyl participating in coordination with a metal, occurs as a result of pi-backbonding from the La³⁺ to the tactmb carboxylate. To examine the porosity of MMCF-3, gas adsorption studies were performed on an activated sample. CO₂ isotherms at 195 K (figure 5) revealed MMCF-3 to retain negligible porosity evinced by a Langmuir surface area of 32 $\text{m}^2 \text{g}^{-1}$, which is presumably due to collapse of the framework after removal of guest solvent molecules.

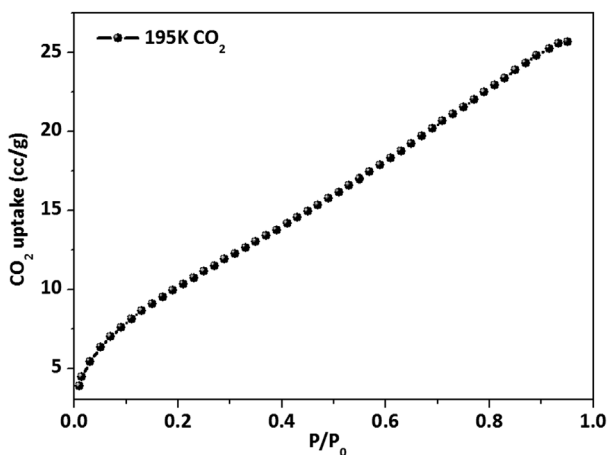
Table 1. Crystal data and structure refinements for MMCF-3.

Empirical formula	C ₄₂ H ₄₈ LaN ₆ O ₁₃
Formula weight	983.77
Temperature (K)	100.15
Crystal system	Monoclinic
Space group	P2 ₁
<i>a</i> (Å)	9.6905(8)
<i>b</i> (Å)	9.7116(8)
<i>c</i> (Å)	21.9727(19)
α (°)	90
β (°)	93.299(2)
γ (°)	90
Volume (Å ³)	2064.4(3)
<i>Z</i>	2
ρ_{calcd} (g cm ⁻³)	1.583
μ (mm ⁻¹)	0.425
<i>F</i> (0 0 0)	1006
Crystal size (mm ³)	0.05 × 0.04 × 0.01
Radiation	Synchrotron ($\lambda = 0.518$)
2θ range for data collection (°)	2.706–36.362
Index ranges	$-11 \leq h \leq 8, -11 \leq k \leq 11, -18 \leq l \leq 25$
Reflections collected	29,780
Independent reflections	6527 [$R_{\text{int}} = 0.0808, R_{\sigma} = 0.0844$]
Data/restraints/parameters	6527/97/582
Goodness-of-fit on F^2	1.051
Final <i>R</i> indexes [$I \geq 2\sigma(I)$]	$R_1 = 0.0593, wR_2 = 0.1386$
Final <i>R</i> indexes [all data]	$R_1 = 0.0891, wR_2 = 0.1521$
Largest diff. peak/hole (e Å ⁻³)	3.05/−1.12
Flack parameter	0.04(3)

Table 2. Selected bond lengths (Å) and angles (°) for MMCF-3.

<i>Bond lengths (Å)</i>			
La53–O21 ^{iv}	2.642(9)	La53–C50 ^{vi}	2.958(15)
La53–O22 ^{iv}	2.570(7)	La53–O51 ^{vi}	2.658(9)
La53–C30 ^v	2.955(16)	La53–O52 ^{vi}	2.561(13)
La53–O31 ^v	2.561(12)	La53–O54	2.544(12)
La53–O32 ^v	2.657(9)	La53–O55	2.513(12)
<i>Bond angles (°)</i>			
O21 ^{iv} –La53–C30 ^v	157.1(4)	O42–La53–C30 ^v	86.2(4)
O21 ^{iv} –La53–O32 ^{iv}	145.4(3)	O42–La53–C50 ^{vi}	157.6(4)
O21 ^{iv} –La53–O42	113.7(3)	O51 ^{vi} –La53–C30 ^v	94.3(3)
O21 ^{iv} –La53–C50 ^{vi}	84.9(4)	O51 ^{vi} –La53–O42	144.4(3)
O21 ^{iv} –La53–O51 ^{vi}	76.3(3)	O51 ^{vi} –La53–C50 ^{vi}	24.6(3)
O22 ^{iv} –La53–O21 ^{iv}	49.6(3)	O52 ^{vi} –La53–O21 ^{iv}	87.2(5)
O22 ^{iv} –La53–C30 ^v	152.7(4)	O52 ^{vi} –La53–O22 ^{iv}	128.6(5)
O22 ^{iv} –La53–O32 ^v	151.9(3)	O52 ^{vi} –La53–C30 ^v	71.3(5)
O22 ^{iv} –La53–O42	75.1(3)	O52 ^{vi} –La53–O32 ^v	79.4(4)
O22 ^{iv} –La53–C50 ^{vi}	112.1(4)	O52 ^{vi} –La53–O42	156.3(4)
O22 ^{iv} –La53–O51 ^{vi}	89.7(3)	O52 ^{vi} –La53–C50 ^{vi}	24.5(4)
C30 ^v –La53–C50 ^{vi}	78.7(4)	O52 ^{vi} –La53–O51 ^{vi}	48.4(3)
O31 ^v –La53–O21 ^{iv}	152.5(5)	O54–La53–O21 ^{iv}	74.7(3)
O31 ^v –La53–O22 ^{iv}	134.6(5)	O54–La53–O22 ^{iv}	115.2(3)
O31 ^v –La53–C30 ^v	24.2(4)	O54–La53–C30 ^v	89.0(4)
O31 ^v –La53–O32 ^v	48.6(3)	O54–La53–O31 ^v	110.2(4)
O31 ^v –La53–O42	91.3(5)	O54–La53–O32 ^v	70.6(3)
O31 ^v –La53–C50 ^{vi}	68.3(6)	O54–La53–O41	65.3(3)
O31 ^v –La53–O51 ^{vi}	76.6(4)	O54–La53–O42	106.7(3)
O31 ^v –La53–O52 ^{vi}	71.3(5)	O54–La53–C50 ^{vi}	89.6(4)
O32 ^v –La53–C30 ^v	24.6(3)	O54–La53–O51 ^{vi}	108.9(3)
O32 ^v –La53–O42	76.9(3)	O54–La53–O52 ^{vi}	66.6(4)
O32 ^v –La53–C50 ^{vi}	94.9(4)	O55–La53–O21 ^{iv}	108.7(3)
O32 ^v –La53–O51 ^{vi}	115.2(3)	O55–La53–O22 ^{iv}	67.6(3)
O41–La53–O21 ^{iv}	76.9(3)	O55–La53–C30 ^v	87.8(4)
O41–La53–O22 ^{iv}	71.4(3)	O55–La53–O31 ^v	67.0(5)
O41–La53–C30 ^v	111.3(4)	O55–La53–O32 ^v	105.9(3)
O41–La53–O31 ^v	130.3(5)	O55–La53–O41	114.5(3)
O41–La53–O32 ^v	88.4(3)	O55–La53–O42	71.6(3)
O41–La53–O42	49.7(3)	O55–La53–C50 ^{vi}	91.3(4)
O41–La53–C50 ^{vi}	152.0(5)	O55–La53–O51 ^{vi}	72.9(3)
O41–La53–O51 ^{vi}	153.2(3)	O55–La53–O52 ^{vi}	113.7(4)
O41–La53–O52 ^{vi}	131.8(4)	O55–La53–O54	176.5(4)

Symmetry codes: (i) $x, 1 + y, z$; (ii) $-1 - x, 0.5 + y, -2 - z$; (iii) $-2 - x, 0.5 + y, -2 - z$; (iv) $x, -1 + y, z$; (v) $-1 - x, -0.5 + y, -2 - z$; (vi) $-2 - x, -0.5 + y, -2 - z$.

**Figure 5.** CO₂ adsorption isotherm of MMCF-3 at 195 K.

4. Conclusion

A metal macrocyclic framework, MMCF-3, was constructed incorporating cyclen units. The vacancy of the macrocycle unit as a coordination site encourages the utilization of the framework as a cation receptor. The availability of these sites allows coordination to newly introduced metals to produce heterometallic frameworks, which may exhibit intriguing properties. Furthermore, though lanthanum may not present the most fascinating properties of the lanthanides, the possibility to exchange the lanthanide atom with more interesting ions, such as Eu^{3+} and Gd^{3+} , exists.

Supplementary material

Details of the synthesis of the H_4Tactmb ligand and powder X-ray diffraction patterns and thermogravimetric plots of MMCF-3 are supplied. CCDC-1449768 contains the supplementary crystallographic data for this paper. These data can be obtained free of charge at <http://www.ccdc.cam.ac.uk/conts/retrieving.html>, or from the Cambridge Crystallographic Data Centre, 12 Union Road, Cambridge CB 21EZ, UK; Fax: (+44) 1223-336-033; or E-mail: deposit@ccdc.cam.ac.uk.

Disclosure statement

No potential conflict of interest was reported by the authors.

Funding

This work was supported by the National Science Foundation [grant number DMR-1352065].

References

- [1] (a) M. Yoon, K. Suh, S. Natarajan, K. Kim. *Angew. Chem. Int. Ed.*, **52**, 2688 (2013); (b) T.R. Cook, Y.R. Zheng, P.J. Stang. *Chem. Rev.*, **113**, 734 (2013); (c) J.J. Perry IV, J.A. Perman, M.J. Zaworotko. *Chem. Soc. Rev.*, **38**, 1400 (2009).
- [2] (a) H.-C. Zhou, J.R. Long, O.M. Yaghi. *Chem. Rev.*, **112**, 673 (2012); (b) H.-C. Zhou, S. Kitagawa. *Chem. Soc. Rev.*, **43**, 5415 (2014); (c) W.-Y. Gao, S. Ma. *Comments Inorg. Chem.*, **34**, 125 (2014); (d) B. Li, M. Chrzanowski, Y. Zhang, S. Ma. *Coord. Chem. Rev.*, **307**, 106 (2016).
- [3] (a) J. Liu, L. Chen, H. Cui, J. Zhang, L. Zhang, C.Y. Su. *Chem. Soc. Rev.*, **43**, 6011 (2014); (b) A.H. Chughtai, N. Ahmed, H.A. Younus, A. Laypkov, F. Verpoort. *Chem. Soc. Rev.*, **44**, 6804 (2015); (c) A. Dhakshinamoorthy, H. Garcia. *Chem. Soc. Rev.*, **43**, 5750 (2014); (d) W.-Y. Gao, H. Wu, K. Leng, Y. Sun, S. Ma. *Angew. Chem. Int. Ed.*, **55**, 5472 (2016).
- [4] (a) L.E. Kreno, K. Leong, O.K. Farha, M. Allendorf, R.P. Van Duyne, J.T. Hupp. *Chem. Rev.*, **112**, 1105 (2012); (b) Z. Hu, B.J. Deibert. *J. Li. Chem. Soc. Rev.*, **43**, 5815 (2014); (c) W.-Y. Gao, S. Palakurty, L. Wojtas, Y.-S. Chen, S. Ma. *Inorg. Chem. Front.*, **2**, 369 (2015).
- [5] (a) Y. Chen, S. Ma. *Rev. Inorg. Chem.*, **32**, 81 (2012); (b) Y. Cui, B. Chen, G. Qian. *Coord. Chem. Rev.*, **273–274**, 76 (2014).
- [6] B. Konig, J. Svoboda. In *Macrocyclic Chemistry: Current Trends and Future Perspectives*, K. Gloe (Ed.), pp. 87–103, Springer, Netherlands (2005).
- [7] Ya. Lampeka, L.V. Tsybal. *Theor. Exp. Chem.*, **40**, 345 (2004).
- [8] H. Zhang, R. Zou, Y. Zhao. *Coord. Chem. Rev.*, **292**, 74 (2015).
- [9] K. Sibbons, K. Shastri, M. Watkinson. *Dalton Trans.*, **5**, 645 (2006).
- [10] B. Geißer, B. König, R. Alsfasser. *Eur. J. Inorg. Chem.*, **6**, 1543 (2001).
- [11] T. Koike, T. Abe, M. Takahashi, K. Ohtani, E. Kimura, M. Shiro. *J. Chem. Soc., Dalton Trans.*, 1764 (2002).
- [12] S. Aoki, H. Kawatani, T. Goto, E. Kimura, M. Shiro. *J. Am. Chem. Soc.*, **123**, 1123 (2001).
- [13] (a) W.-Y. Gao, Y. Niu, Y. Chen, L. Wojtas, J. Cai, Y.-S. Chen, S. Ma. *Cryst. Eng. Comm.*, **14**, 6115 (2012); (b) W.-Y. Gao, Y. Chen, Y. Niu, L. Cash, P. Perez, L. Wojtas, J. Cai, Y.-S. Chen, S. Ma, *Angew. Chem. Int. Ed.*, **53**, 2615 (2014); (c) W.-Y. Gao, K. Leng, L. Cash, M. Chrzanowski, C.A. Stackhouse, Y. Sun, S. Ma. *Chem. Commun.*, **51**, 4827 (2015).
- [14] Bruker. *APEX2 (Version 2013.6-2)*, Bruker AXS Inc., Madison, Wisconsin, USA (2010).
- [15] Bruker. *SAINT-V8.32A, Data Reduction Software*, Bruker AXS Inc., Madison, Wisconsin, USA (2009).
- [16] G.M. Sheldrick. *SADABS, Program for Empirical Absorption Correction*, University of Gottingen, Germany (1996).
- [17] (a) G.M. Sheldrick. *Acta Cryst.*, **A46**, 467 (1990); (b) G.M. Sheldrick. *Acta Cryst.*, **A64**, 112 (2008).
- [18] O.V. Dolomanov, L.J. Bourhis, R.J. Gildea, J.A.K. Howard, H. Puschmann. *J. Appl. Cryst.*, **42**, 339 (2009).
- [19] A.L. Spek. *Acta Cryst.*, **D65**, 148 (2009).